6.9 Skill of an aircraft wake-vortex transport and decay model using weather prediction and observation

Michael Frech* **and Frank Holzäpfel**
Institut für Physik der Atmosphäre
Deutsches Zentrum für Luft- und Raumfahrt (DLR) Oberpfaffenhofen
D-82234 Weßling, Germany

1. Introduction

In order to safely reduce aircraft separation during approach and landing, the wake vortex behavior along the glide path has to be known and predicted. This requires in principle the knowledge of wake vortex relevant meteorological parameters along the entire glide path where typically continuous meteorological measurements of all relevant variables are not feasible. For multiple purposes a one-year meteorological data base for the Frankfurt Terminal area has been generated using NOWVIV. The skill of the nowcasting system NOWVIV (Nowcasting Wake Vortex Impact Variables, Gerz et al. 2005) to predict these environmental parameters is assessed. This one-year data set comprises typical weather conditions and includes already typical features of a long-term surface wind climatology. It enables to test new operational concepts with realistic meteorological input and to estimate the potential for aircraft separation reduction. It may also be used within risk assessments for prototype wake-vortex advisory systems (Gerz et al. 2005).

A subset of the one-year data base is analysed in detail for a period of 40 days where a dedicated wake measurement campaign was carried out at Frankfurt airport in fall 2004 (Frech et al., 2005). In total 231 wake vortex pairs generated by heavy aircraft in ground proximity were tracked and characterized by LIDAR. During this measurement campaign a SODAR/RASS and a LIDAR provided profile measurements of meteorological variables. These data are used to analyse the quality of the predicted profiles of wind, temperature and turbulence (Frech et al., 2005). Furthermore we carry out a skill analysis to investigate the potential of NOWVIV as a real-time prediction system where we focus on the ability to predict pre-defined cross wind thresholds. The skill of NOWVIV is compared to the skill of a simple cross wind persistence model based on SODAR measurements. For this purpose we assume that a given measured cross wind profile is valid over the whole forecast lead time and evaluate the skill of the forecast with increasing lead time every 10 minutes.

In a wake-vortex advisory system, the weather prediction and observation system is coupled to a wake vortex predictor. Therefore, we have to know how the predictive skill of the weather forecast system influences the predictive skill of the whole forecast system chain including the wake predictor. Consequently, we extend this analysis by coupling the Probabilistic Two-Phase wake vortex transport and decay model P2P (Holzäpfel, 2003) to the NOWVIV system and investigate the predictive skill of P2P for pre-selected confidence levels of vortex position and strength. The skill is assessed by comparing the predictions against LIDAR measured wake vortex position and strength. Initially, the overall skill of the wake vortex forecast is analysed. We then analyse the skill of the models with respect to observed and predicted clearance of a safety corridor from wake vortices (WV). In particular, we focus on the frequency of non-conservative predictions, which refer to a situation where a wake vortex is predicted to be outside a predefined safety corridor while observations still indicate the presence of a wake

*Corresponding author address: Michael Frech, Institut für Physik der Atmosphäre, DLR Oberpfaffenhofen, D-82234 Weßling, Germany. Email: Michael.Frech@dlr.de

vortex in the safety corridor. A non-conservative predictions refers to a potential risk for a following aircraft which has to be avoided.

2. The model system NOWVIV

A hierarchy of weather forecast models is combined within the model system "NOWVIV" - NOwcasting Wake Vortex Impact Variables. The core of NOWVIV is the mesoscale model MM5 (Grell et. al, 2000) where a Yamada & Mellor 2.5 level turbulence closure scheme is employed from which TKE is computed as a prognostic variable. Two nested domains with sizes of about 250x250 km^2 and about 90x90 km^2 centered on Frankfurt airport with grid distances of 6.3 km and 2.1 km, respectively, are used. The model employs 60 vertical levels such that in the altitude range of interest ($z < 1100$ m above ground) 26 levels yield a vertical resolution varying between 8 m and 50 m. Initial and boundary data are taken from the numerical data assimilation model LM (Lokal Modell) of DWD (German Weather Service).

Detailed terrain and landuse information is provided to NOWVIV. NOWVIV is initialized every 12 hours, 12 UTC and 0 UTC. Locally measured data have not been assimilated for this test. Output variables are vertical profiles of horizontal and vertical wind, u, v, w, virtual potential temperature θ_v and turbulent kinetic energy e.

3. Measurement campaign

The Frankfurt measurement campaign represents an unique opportunity to assess a subset of the NOWVIV climatology in more detail by using sonic anemometer and SODAR/RASS measurements. We focus here on a data comparison for 40 days (26.8.2004 until 5.10.2004). The measurements were taken at a site close to the runway threshold of 25L/R (Figure 1). This time period includes a whole range of synoptic conditions, from late summer high pressure situations to frontal passages with strong winds and precipitation.

The SODAR/RASS measurements provide 10-minute averaged profiles of all three wind components, standard deviations of vertical velocity and virtual temperature. The vertical resolution of the profiles is 20 m, and the

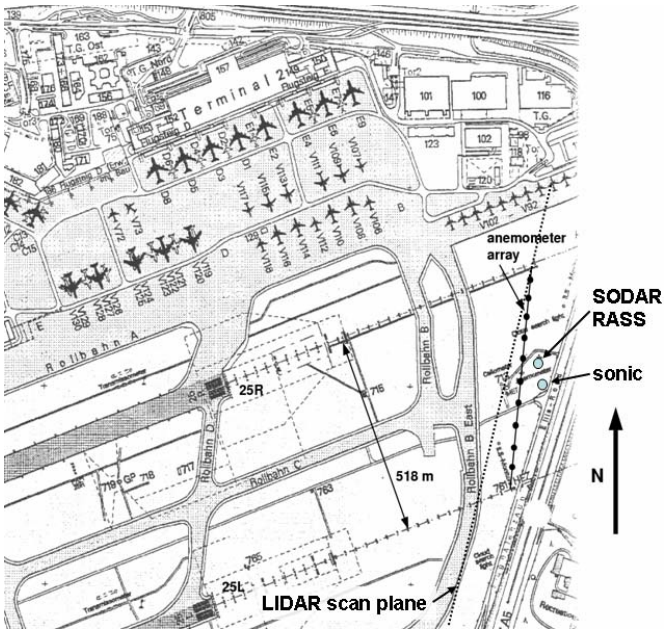

Figure 1: Layout of sensor location near the thresholds of runway 25L/R. Also shown is the DFS anemometer array and the DLR LIDAR scan plane.

first measurement level is 40 m (which represents an average between 30 m and 50 m). The vertical availability of meteorological parameters varies with time, depending on environmental (aircraft noise) and meteorological conditions. With the chosen settings, the vertical availability of SODAR/RASS data is typically on the order of 200-300 m. The accuracy of the wind speed measurement depends on the wind speed magnitude. Up to 5 m/s the accuracy is within ± 0.5 m/s and from 5 - 35 m/s within $\pm 10\%$. For wind direction, the accuracy is $\pm 5°$. The standard deviation of vertical wind velocity can be estimated within ± 0.15 m/s. In addition an ultra-sonic anemometer at z=10 m was operated close to the SODAR/RASS measurements. The sonic anemometer provides measurements of all three wind components and temperature at a sampling rate of 17 Hz.

In total 231 wake vortex pairs generated by A340 and B747 aircraft during final approach at a nominal height of about 60 m above the ground were traced with a 2-

μm pulsed lidar system. The lidar scanned the measurement plane in an angle of 123° to flight direction employing elevation sectors of 0° to 15°. For the evaluation of wake-vortex properties, an interactive four-stage data processing algorithm was applied which is described in detail in Köpp et al. (2004). From estimated profiles of vortex tangential velocities vortex positions and circulations were derived.

4. Probabilistic wake-vortex prediction model

The real-time Probabilistic Two-Phase aircraft wake-vortex model (P2P) considers all of the first order WV impact parameters, namely the aircraft configuration, wind, turbulence, temperature stratification, wind shear, and proximity of the ground. Detailed descriptions, applications, and assessments of P2P are available in Holzäpfel (2003, 2005), Holzäpfel and Robins (2004), and Holzäpfel and Steen (2006). The model is formulated in normalized form where the characteristic scales are based on initial vortex separation, b_0, and circulation, Γ_0, leading to the time scale $t_0 = 2\pi {b_0}^2/\Gamma_0$.

For the prediction of circulation, the concept of two-phase circulation decay is pursued, where a turbulent diffusion phase is followed by a rapid decay phase (see Fig. 2). This behavior has been adopted from large eddy simulation results of wake vortex evolution in turbulent and stably stratified environments and, in the meantime, has also been confirmed by lidar observations (Holzäpfel, 2004). Aloft the onset time of rapid decay depends on ambient turbulence and stratification. In ground proximity, however, the decay rate is mainly controlled by the interaction of the wake vortex with secondary vortices which detach from the boundary layer at the ground. Consequently, in ground effect the decay rate depends only weakly on ambient meteorological conditions. On the other hand, the impact of cross wind on vortex rebound characteristics is very strong. Cross wind attenuates (intensifies) the formation of the luff (lee) secondary vortex which causes pronounced asymmetric rebound behavior (see Fig. 2).

To consider spatiotemporal variations of vortex position and strength, which are caused primarily by tur-

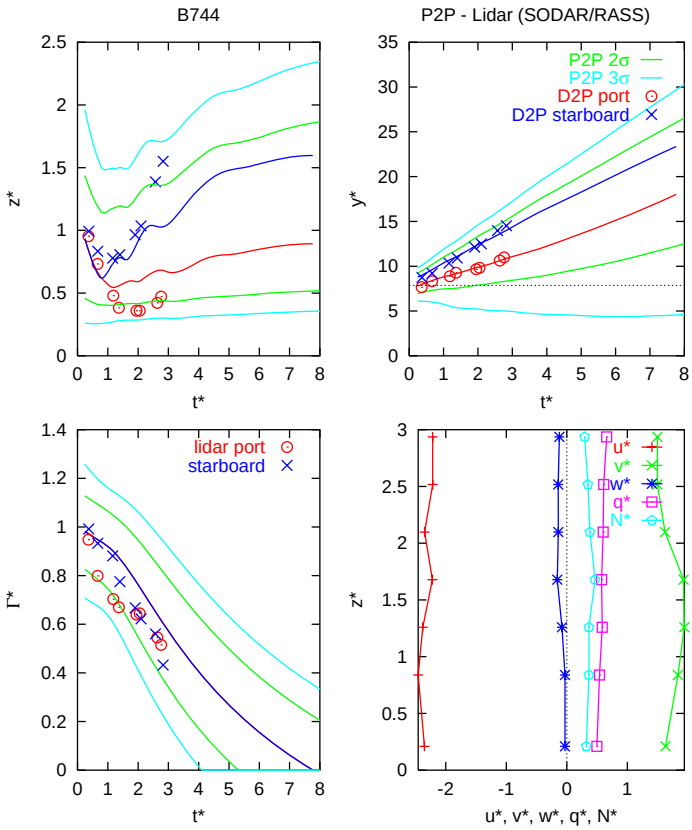

Figure 2: P2P predictions with SODAR/RASS input. Measured (symbols) and predicted (lines) evolution of normalized vertical and lateral positions, z^*, y^*, and circulation, Γ^*, in ground proximity. Red and blue lines denote deterministic behavior, green and light blue lines envelopes for probabilities of 95.4% and 99.73%, respectively. Right below, vertical profiles of normalized environmental data.

bulent transport and deformation processes, the probabilistic model predicts WV behavior within defined confidence intervals (see Fig. 2). For this purpose, decay parameters are varied in consecutive model runs and various static and dynamic uncertainty allowances are added which consider the increased scatter of wake vortex position and strength in turbulent environments and their modified trajectories caused by tilting and rebound in wind shear situations. The obtained probabilistic envelopes can be adjusted to represent arbitrary degrees of probability. The respective envelopes are estimated based on a training procedure (Holzäpfel, 2005) that relates the predicted envelopes to field measurement data. To achieve consistency in between wind and wake prediction skill, separate fits are used for wake predictions driven by predicted and by measured environmental parameters. A deterministic model version termed D2P provides mean wake vortex evolutions employing intermediate decay parameters.

Figure 2 displays an extreme example where the asymmetric rebound is very pronounced such that evolutions of vertical vortex position exceed the 2σ-envelopes (95.4 %). Figure 3 shows the same overflight based on a relatively poor NOWVIV cross wind prediction. Note, that the spread of the probabilistic envelopes for lateral position, y^*, is increased compared to the SODAR driven predictions due to cross wind prediction uncertainties.

5. Weather and Wake Vortex forecast performance

The weather forecast performance is evaluated based on 40 days of measurements. The RMS error and bias of wind speed and direction is shown in figure 4. Overall we find no systematic bias in wind direction and speed. The RMS error of wind speed increases with height from 1.5 m/s to about 2.5 m/s. The corresponding RMS error of wind direction varies between 40 to 45°. In addition, we show also the first and third quartile of the error distribution. The 1st and 3rd quartile profiles both indicate deviations on the order of 20° which indicates that the RMS error appears to be dominated by large outliers. Overall, the results suggest a good forecast performance compared to statistics published in literature (e.g. Zhong

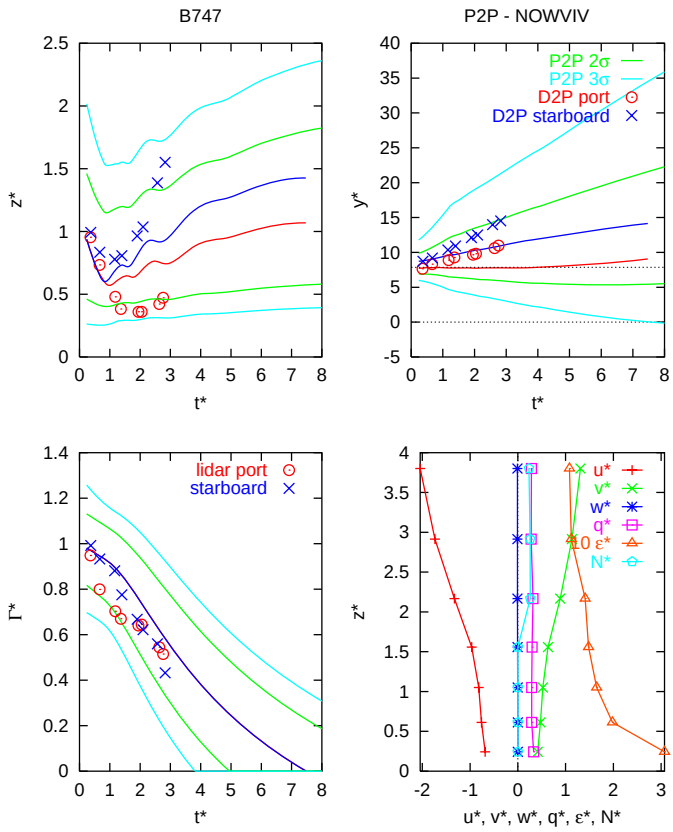

Figure 3: P2P predictions with NOWVIV input (see also the same overflight in figure 2).

et al., 2005).

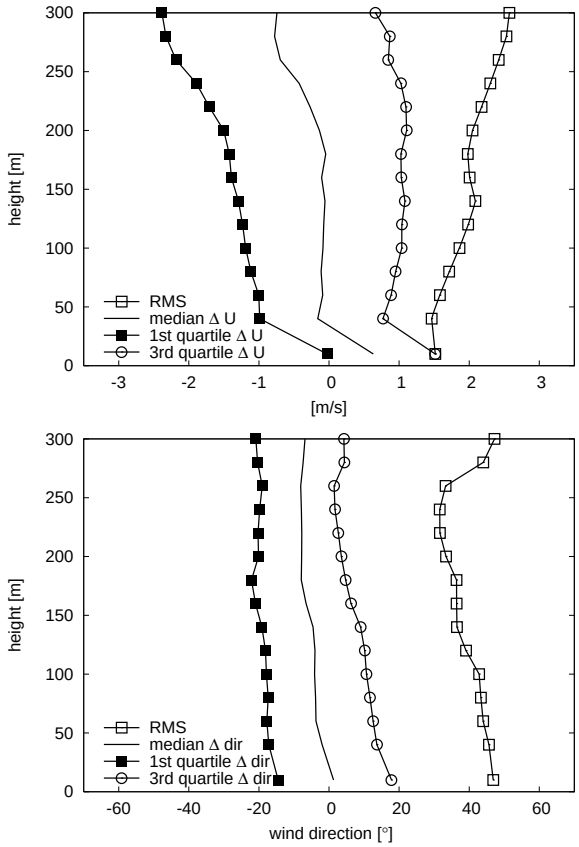

Figure 4: Root-mean square error and mean bias of wind speed and direction.

In ground proximity cross wind driven wake vortex drift constitutes the primary mechanism to clear the approach corridor from wake vortices. For an operational wake-vortex advisory system the correct timing of cross wind predictions is decisive. We therefore extend this analysis by comparing the model forecast not only against observations but also against a cross wind prediction based on a simple persistence forecast. For analysis purposes we consider a forecast lead time of up to 6 hours in order to identify the lead time for which we can expect a superior model forecast. The cross wind thresholds considered are 2 and 3 m/s, respectively. The requirement is, that the exceedance of a given cross wind threshold has to be predicted correctly over the whole cross wind profile. From a contingency table we compute the false alarm rate (FAR, e.g Nurmi, 2003). A false alarm refers to a situation, where the predicted cross wind is above the threshold whereas the measured cross wind is below the specified cross wind threshold. The result is shown in Figure 5. The FAR increases with increasing cross wind threshold. The FAR of NOWVIV is 0.2 (0.32) for a cross wind threshold of 2 m/s (3 m/s). We find that the skill of the persistence forecast up to a lead time of 60 min (80 min) is superior compared to the NOWVIV performance. Beyond this lead time, NOWVIV shows a better forecast performance. Clearly the non-stationary diurnal evolution of the boundary layer wind cannot be captured by a persistence assumption.

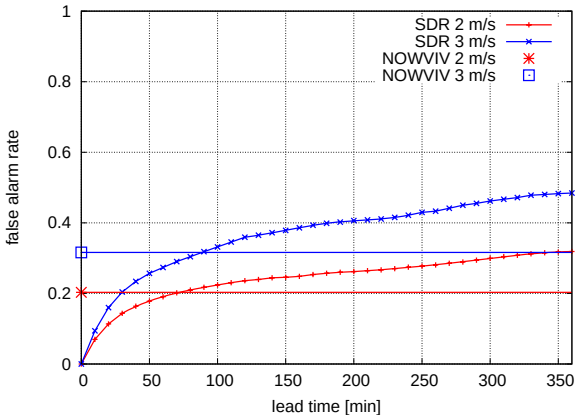

Figure 5: The False Alarm Rate regarding exceedance of cross wind thresholds of 2 and 3 m/s for a SODAR persistence forecast and the NOWVIV forecast based on 40 measurement days.

It has to be noted that we use the direct model output without any further optimization by using e.g. local observations. An approach referred to as Model Output Statistics (MOS) is commonly employed by weather services to correct direct model output and to assign confidence levels to forecasted parameters. Certainly, there is potential to reduce the NOWVIV FAR by introducing safety allowances based on our knowledge of the error characteristics. Here the dependence of the error on the prevailing synoptic situation, the wind direction (runway parallel or not) could be used to identify situations

where the model output requires smaller or larger safety allowances.

To investigate effects regarding the impact of meteorological data on wake-vortex behavior as it is done within a wake vortex advisory system, we couple the NOWVIV forecast and SODAR measurements with the P2P wake vortex model.

We first analyse the overall forecast performance of P2P using NOWVIV and the simple persistence forecast as input. We employ a scoring procedure which considers in total 231 high quality wake vortex measurements serving as a reference for the evaluation of the P2P results. The scoring procedure evaluates the root mean square deviations of measurement and prediction of the quantities y^*, z^*, and Γ^* for each overflight. From the distribution of rms values resulting from the 231 cases, the median and the 90th percentile are used to characterize the performance of the models. The classical scoring approach is based on a deterministic version of P2P (D2P) whereas an operational system would employ the fully probabilistic version of P2P.

The scoring results shown in figure 6 indicate that the D2P predictions of the lateral WV position using NOWVIV input initially are about a factor of two larger than the predictions using SODAR input. For a typical large aircraft with an initial vortex spacing of $b_0 = 45$ m, the RMS error of the lateral vortex position using SODAR input is on the order of 20 m. For completeness we also show the 90th percentile of the RMS error distribution which displays similar characteristics as the median (figure 6, lower panel). The 90th percentile for the SODAR driven prediction is near $y^* = 1$ and $y^* = 2.1$ for the NOWVIV case.

As one could expect the RMS error of lateral position increases with increasing lead time using the SODAR based persistence model. The cross over time is found for a lead time of $t_{lead} \approx 60$ min which approximately corresponds to the cross over time we found for a cross wind threshold of 2 m/s with respect to FAR (see figure 5).

The RMS errors of the vertical position are for both numerical prediction and persistence forecast nearly identical which suggests that the vertical position of the wake vortex is dominated by the interaction with the solid surface which is also reflected by the fact that the error is essentially constant with increasing lead time. For circulation we obtain a similar behavior which can be attributed to the weak dependence of wake vortex decay in ground effect to meteorological parameters.

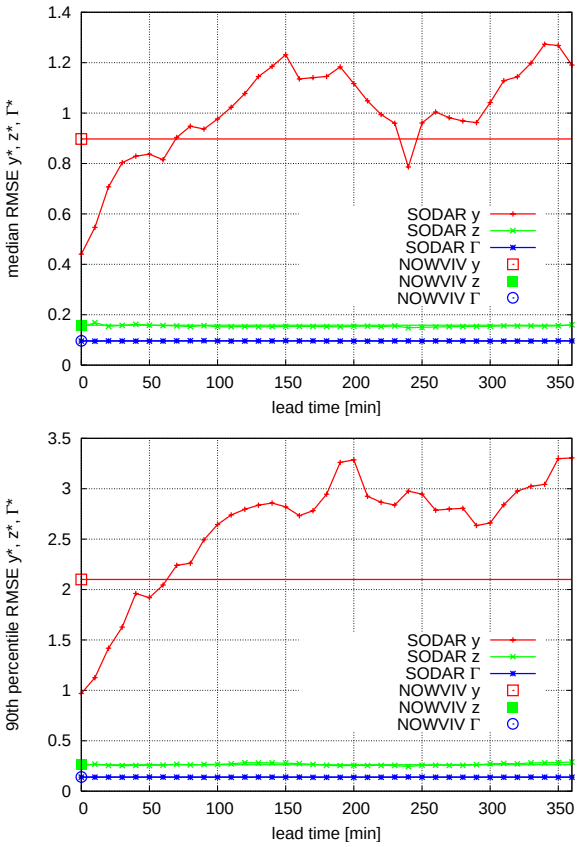

Figure 6: Median (upper panel) and 90th percentile (lower panel) of the normalized root-mean square error distribution of the predicted lateral and vertical wake vortex position and circulation.

In principle one could expect that the error in lateral WV position is directly correlated to the cross wind error. This dependence is shown in figure 7 where the NOWVIV RMS error of cross wind for each WV observation is plotted against the RMS error of the corresponding WV position. A clear relation between the NOWVIV RMS error of cross wind and lateral position cannot be found. There appears to be a weak tendency that an increasing NOWVIV RMS error of cross wind leads to increasing

errors in predicted lateral position.

In order to understand this we refer to figure 6 which shows that also SODAR driven P2P does not yield perfect predictions of lateral transport. This implies that the SODAR measured wind profile is only approximately representative for the volume of air in which the wake evolves. This is partly due to the time required for averaging in order to obtain a realistic wind profile and because of the distance of the sensor to the wake trajectory ($\approx$ 300 m). If we would have a perfect wind measurement we could hope for a negligible error in the prediction of lateral wake position. But more important, the interaction of the wake with its environment leads to complex 3-D deformations and spatially varying decay processes such that we have to expect significant variability of vortex strength and position in particular for older wake ages (e.g. Holzäpfel et al., 2000). All these aspects contribute to the very weak correlation between the RMS cross wind error and the error in lateral position in figure 7. Such findings motivated the development of the probabilistic wake vortex transport model P2P, realizing that deterministic model approaches would never succeed in describing the 3-D nature of wake vortex evolution in the atmosphere.

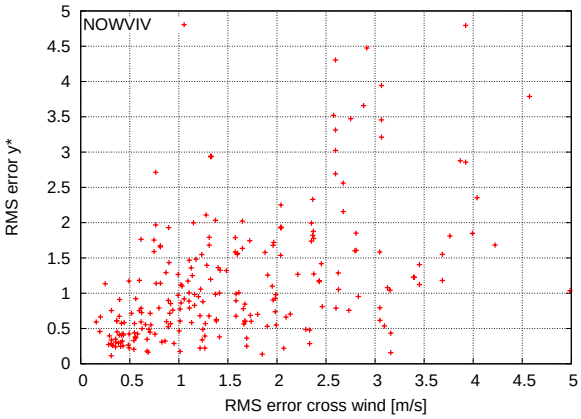

Figure 7: NOWVIV RMS error of cross wind versus the corresponding RMS error of the predicted normalized lateral wake vortex position for individual overflights.

Previous analysis concentrated on the skill of the deterministic version of P2P compared to Lidar measured wake vortices. We now focus on the performance of the fully probabilistic version of the model to predict the time when a wake vortex leaves a safety corridor, t_l. The requirement is that $t_{l,observed} \leq t_{l,predicted}$. We employ the dimensions of the safety corridor defined in the Wake Vortex Warning System developed by DFS (Gurke and Lafferton, 1997). The corridor has a width of $\pm$45 m from the runway centerline. In the analysis we consider only WVs that were observed by the Lidar at least for 60 s, so that 7 wake measurements had to be removed from the sample.

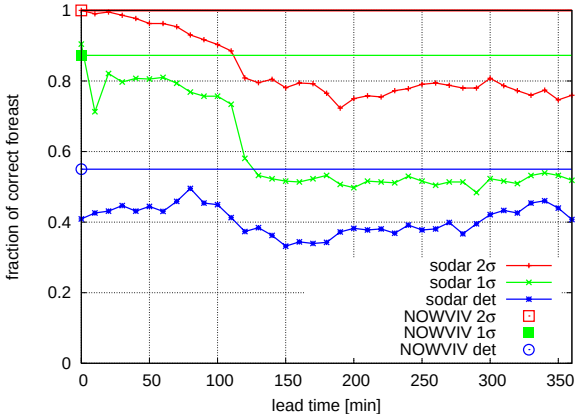

Figure 8: The fraction of model forecasts which correctly predicts the time to leave the corridor, t_l. The requirement is that $t_{l,observed} \leq t_{l,predicted}$. Shown are P2P results using 1σ and 2σ-confidence levels, and D2P (det) results using SODAR and NOWVIV input.

Within figure 8 the best skill is obtained using P2P predictions with 2σ-confidence level (95.4%). There both SODAR and NOWVIV driven P2P versions demonstrate nearly equal skill at $t_{lead} = 0$. Both forecasts show a perfect performance of 100% conservatively predicted time to leave the corridor. For a lead time of 30 min, the persistence approach (SODAR-P2P) still correctly predicts the residence time in 99% of the cases. It is remarkable that NOWVIV input leads to comparable skill compared to e.g. the previously analyzed FAR. This can be attributed to the P2P safety allowances which were adopted to the NOWVIV predictions and thus lead to acceptable results even for inaccurately predicted meteorological input. The quality of the P2P forecast driven by SODAR starts to degrade substantially for lead times

beyond $\approx$ 60 minutes which is consistent with previous results. If we consider a confidence level of 1σ (68.3%), the quality of the forecast for both inputs is still remarkably well ($\approx$ 90%). Compared to the 2σ-confidence level result, the skill of the P2P 1σ-confidence level shows a similar dependence for increasing lead time. For illustrative purposes we show the deterministic version of P2P which indicates a rather poor performance in predicting the correct safe residence times. This is not surprising as D2P is optimized to predict the individual wake behavior as close as possible to the observations such that a predicted residence time may be often very close to the actual residence time but eventually be too low. This will be investigated in more detail below. The analysis clearly illustrates that the probabilistic approach is needed in order to capture the large variability of wake vortex evolution.

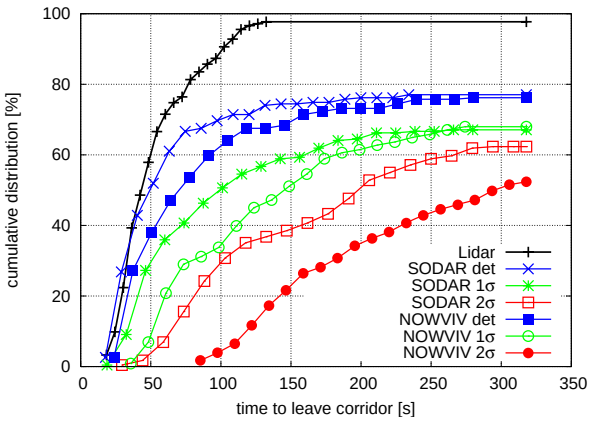

Figure 9: Cumulative distribution of time to leave the corridor based on observations (Lidar) and P2P predictions (deterministic and varying probability levels) using NOWVIV and SODAR input.

The high level of skill shown in figure 8 needs to be assessed together with the associated predicted times to leave the corridor, which describe the related potential runway capacity increase. For this purpose we have computed cumulative distributions of the time needed to clear a safety corridor from wake vortices using P2P runs with different input and confidence levels, and the Lidar observations (figure 9). The cumulative distribution based on Lidar observations indicates that most of the measured wakes have left the corridor within $\approx$ 120 s. Only three wakes remain in the corridor. The cumulative distribution based on the deterministic forecasts suggests that at that time only 71% of the wakes have left the corridor, while in total (at $t = 320$ s) 25% of the predictions suggest that the wakes remain in the corridor. This fraction is increasing up to 45% with increasing confidence level for both the NOWVIV and SODAR driven P2P forecast. If we consider the 120 s threshold 55% (45%) of the wakes based on the 1σ, and 36% (11%) for the 2σ-confidence level have left the corridor employing the Sodar (NOWVIV) P2P forecast. This figure suggests, that there is potential to reduce separation even for the NOWVIV-P2P 2σ confidence level forecast, even though it appears rather small. Note that previous discussion also has to consider the fact, that LIDAR observes vortex behavior only within the observation plane which means that not all parts of the deformed vortices may have actually left the safety corridor at the times indicated in figure 9. This implies that the actual percentage of wakes, which have left the corridor at a given time, is likely to be lower as analyzed from the Lidar observations. This means that the actual potential capacity gain is lower than suggested by the Lidar data in figure 9. In contrast, the probabilistic predictions specify that all parts of the vortices have left the corridor.

The cumulative distribution based on the deterministic SODAR-D2P forecast suggests that there are non-conservative deterministic predictions for the time to leave corridor below 30 s. This is evaluated by computing the corresponding histogram of the difference between observed and predicted time to leave the corridor $\Delta t_l = t_{l,LIDAR} - t_{l,prediction}$ (see Fig. 10, upper panel). In addition the histogram for the 2σ-level predictions is shown in the lower panel of figure 10.

The histogram for the deterministic SODAR-D2P results indicates that most of the forecasts are close to the observations. Neglecting time differences below $\Delta t_l = -50$ s, we find quasi normal distribution around $\Delta t_l = 0$ s. The deterministic NOWVIV-D2P results show also a normal distribution with a larger width. These histograms explain the apparently rather poor performance of D2P shown figure 8 where positive Δt_l shown in the upper panel of figure 10 cause the large fraction of incorrectly predicted times to leave the corridor. The histograms for the P2P runs with 2σ-confidence level show

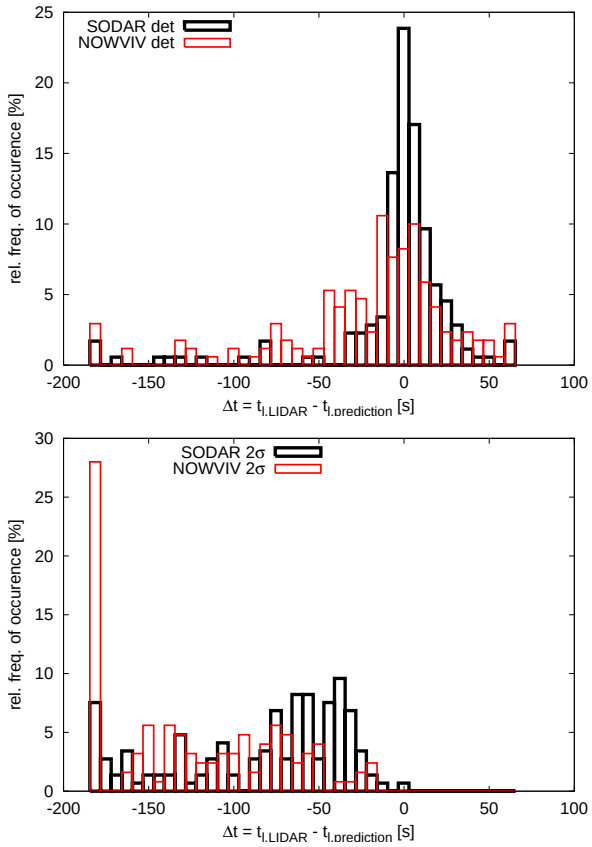

Figure 10: Histograms of the difference between observed and predicted time to leave the corridor ($t_{l,LIDAR} - t_{l,prediction}$) for deterministic predictions above and probabilistic predictions below.

for both SODAR and NOWVIV driven P2P no forecast with $\Delta t_l > 0$ s which indicates a high level of safety of the predictions. On the other hand, the histogram also suggests the necessity to use a 2σ-confidence level as there are no predictions with $\Delta t_l > 0$ in contrast to the findings for P2P runs with a 1σ-confidence level (not shown).

6. Summary

In this paper we have shown the performance of the real-time wake vortex prediction and transport model P2P using observed and predicted meteorological data as input taken at Frankfurt airport in fall 2004. The predicted meteorological profiles are based on the nowcasting model NOWVIV which are compared against predictions applying a simple persistence assumption up to a lead time of 6 hours. In general, the meteorological profiles compare well with the SODAR/RASS observations. The skill of NOWVIV to predict a pre-defined cross wind threshold is assessed in terms of the False Alarm Rate which indicates a better prediction skill compared to the persistence forecast after a lead time of about 70 min. We find a false alarm rate between 0.2-0.3. Without optimizing the NOWVIV forecast by introducing e.g. a MOS-type approach, we use the predicted and observed meteorological profiles as input to P2P. The skill of P2P using those input data is assessed by a scoring procedure. Initially, the RMS error of NOWVIV-P2P predictions of lateral position are about a factor of two larger than the SODAR-P2P results. Independent of cross wind magnitude, we find a better NOWVIV-P2P prediction performance compared to the persistence assumption beyond a lead time of 60-70 minutes. This result refers to the use of the deterministic version of P2P where the predictions are directly compared to the LIDAR measurements. Considering 1σ- and 2σ-confidence levels and analysing the time it takes to transport a wake out of the safety corridor, P2P provides very safe forecasts for both NOWVIV and SODAR input. This is a very promising result which suggests that model forecast can be used even at early lead times. However, considering the cumulative distribution of the corresponding time to leave the corridor, the use of 2σ-confidence levels shows a rather conservative predictive behavior compared to the actual LIDAR measured time to leave the corridor. Nevertheless, there appears potential to reduce aircraft separation based on wake vortex prediction. In a next step this analysis needs to be performed also for measurements out-of-ground effect in order to check whether similar results are obtained. Furthermore the benefit of other meteorological data sources such as AMDAR data will be investigated. An important aspect is the assessment and consideration of the spatial variability of meteorological parameters along the glide path.

Acknowledgment: We gratefully acknowledge the excellent support and work of the teams from Airbus, DFS

Deutsche Flugsicherung GmbH, DLR, Fraport AG and METEK during the measurement campaign.

References

Frech, M., Tafferner, A, Holzäpfel, F., and Gerz, T.: 2005: High resolution weather data base for Frankfurt airport, to be submitted *Journal of Applied Meteorology*.

Gerz, T., Holzäpfel, F., Bryant, W., Köpp, F., Frech, M., Tafferner, A., and Winckelmans, G., 2005: Research towards a wake-vortex advisory system for optimal aircraft spacing, *Comptes Rendus Physique*, Academie des Sciences, Paris **Vol. 6, No. 4-5**, pp. 501-523.

Grell, G., Schade, L., Knoche, R., Pfeiffer, A. and Egger J., 2000: Nonhydrostatic climate simulations of precipitation over complex terrain, *J. Geophys. Res.*, **105(D24)**, 29595-29608.

Gurke,T. and Lafferton, H., 1997: The Development of the Wake Vortices Warning System for Frankfurt Airport: Theory and Implementation, *Air Traffic Control Quarterly*, **5(1)**, pp. 3-29.

Holzäpfel, F., Gerz, T., Frech, M. and Dörnbrack, A., 2000: Wake Vortices in a Convective Boundary Layer and Their Influence on Following Aircraft, *J. Aircraft*, **Vol. 37, No.6**, pp. 1001-1007.

Holzäpfel F., 2003: Probabilistic Two-Phase Wake Vortex Decay and Transport Model, *J. Aircraft*, **Vol. 40, No. 2**, pp. 323-331.

Holzäpfel F., Robins R.E., 2004: Probabilistic Two-Phase Aircraft Wake-Vortex Model: Application and Assessment, *J. Aircraft*, **Vol. 41, No. 5**, pp. 1117-1126.

Holzäpfel F., 2005: Probabilistic Two-Phase Aircraft Wake-Vortex Model: Further Development and Assessment, Report No. 207, Institut für Physik der Atmosphäre, accepted for publ. in *J. Aircraft*.

Holzäpfel F., Steen M., 2006: Aircraft Wake-Vortex Evolution in Ground Proximity: Analysis and Parameterization, *AIAA Paper 2006-1077*, Jan 2006.

Köpp, F., Rahm, S., and Smalikho, I., 2004: Characterization of Aircraft Wake Vortices by $2-\mu\mathrm{m}$ Pulsed Doppler Lidar, *Journal of Atmospheric and Oceanic Technology*, **Vol. 21, No. 2**, pp. 194–206.

Nurmi P., 2003: Recommendation on the verification of local weather forecasts, ECMWF Tech. Mem. 430, 21pp.

Zhong S., Hee-Jin, I., Bian, X., Charney, J., Heilman, W., and Potter B., 2005: Evaluation of Real-Time High-Resolution MM5 Predictions over the Great Lakes Region, *Weather and Forecasting*, **Vol. 20**, pp. 63–81.